

THE VISCOELASTIC CONTACT BETWEEN HIGH-ORDER POLYNOMIAL SURFACES

Sergiu Spinu^{1,2}, Delia Cerlinca^{1,2}

¹ Department of Mechanics and Technologies, Stefan cel Mare University of Suceava, 13th University Street, 720229, Romania, e-mail: sergiu.spinu@fim.usv.ro, delia@fim.usv.ro

² Integrated Center for Research, Development and Innovation in Advanced Materials, Nanotechnologies, and Distributed Systems for Fabrication and Control (MANSiD), Stefan cel Mare University, Suceava, Romania.

Abstract: The improvement of the load-carrying capacity of machine elements subjected to contact load can make use of high-order surfaces, providing a central plateau of uniform pressure surrounded by a peripheral region of pressure continuously decreasing to zero. The solution of the viscoelastic contact problem is difficult to obtain because (1) both contact area and pressure distribution are a priori unknown, and (2) the contact parameters keep changing with time. The latter difficulties are overcome in this paper by conducting numerical analysis based on both spatial and temporal model discretization. The strong points of the newly proposed algorithm consist in: (1) the ability to incorporate complex models of viscoelasticity, (2) the capability to treat arbitrary contact geometry, and (3) the capacity to simulate arbitrary loading histories. The history of pressure distribution, as well as evolution of contact area and of the rigid-body approach in the contact between a rigid indenter bounded by high-order polynomial surfaces and a polymethyl methacrylate viscoelastic half-space, are obtained. These results prove the advantages of high-order surfaces for the contact in the viscoelastic domain.

Keywords: numerical simulation, viscoelastic displacement, high-order polynomial surfaces

1. Introduction

The design of mechanical contacts involving machine elements made by viscoelastic matrix and bounded by high-order surfaces can be improved by numerical analysis. The latter can overcome the limitations existing in most analytical solutions: (1) the constitutive law of the contacting material is usually elastic, and (2) the contact geometry is quadratic, thus obeying the Hertz contact theory.

Hasslinger [1] proved that the optimal load-carrying capacity of the mechanical contact can be attained with a uniform pressure over the whole contact area. The latter configuration is incompatible with Linear Elasticity, which requires continuity of stresses in order to fulfill the compatibility conditions. The solution is to admit a peripheral region of

pressure continuously decreasing to zero, bordering a central plateau of uniform pressure. The latter pressure distribution cannot be achieved in the frame of the Hertz contact, which exhibits a semi-ellipsoidal pressure distribution. However, the shape parameters of indenters bounded by high-order polynomial surfaces can be chosen to flatten the pressure distribution in central zone of contact area.

The closed-form equations for the contact involving high-order surfaces were developed by Diaconescu [2]. Diaconescu and Glovnea [3] further derived the correlation between pressure distribution and the equation of high order axisymmetric surfaces and established a procedure to flatten the pressure distribution in the central zone of contact area. More recently, these authors [4] further derived the indenter equations which lead to an optimized pressure

distribution in the elliptical contact, and provided a numerical validation of the theoretical framework. Spinu and Gradinaru [5] investigated the load-carrying capacity of the contact between high-order surfaces under conditions of gross-slip and partial-slip. However, all these research efforts were limited to the elastic domain.

In this paper, a more in-depth study of this remarkable type of surfaces is conducted, by analyzing the pressure developing in the contact between bodies made by linear viscoelastic matrix, bounded by fourth and sixth-order surfaces. To this end, a technique originally developed for the elastic contact of rough bodies [6] is combined with a method for viscoelastic displacement computation [7].

2. The contact of high-order surfaces

General formulae governing the elliptic contact of high-order surfaces were derived by Diaconescu [2]. The latter author obtained the polynomial punch profiles that induce the following pressure distributions:

$$p(\rho) = p_0 \sqrt{1-\rho^2} \sum_{i=0}^{n-2} c_i \rho^{2i}, \quad (1)$$

$$c_0 = 1, \quad c_i = \frac{2i-1}{2i} c_{i-1},$$

where p_0 is the central pressure, n the degree of the polynomial expressing the corresponding punch profile, x and y the system coordinates in the common plane of contact, and $\rho^2 = x^2 a^{-2} + y^2 b^{-2}$, with a and b the contact area half-axes.

In this framework, the fourth order polynomial surface that induces an axisymmetric pressure distribution, possessing a flat central pressure plateau surrounded by a monotonous decrease to zero, can be expressed [3] in a radial coordinate system as:

$$hi(r) = \frac{3}{128} \pi \eta p_0 a \left[8 \left(\frac{r}{a} \right)^2 + 3 \left(\frac{r}{a} \right)^4 \right], \quad (2)$$

with p_0 the central pressure induced by a normal load W , with $p_0 = 5W/(4\pi a^2)$. The optimized pressure distribution induced by a punch of equation (2) is [3]:

$$p(\rho) = p_0 \sqrt{1-\rho^2} \left(1 + \frac{1}{2} \rho^2 \right). \quad (3)$$

In the same manner, an optimized pressure distribution of the form:

$$p(\rho) = p_0 \sqrt{1-\rho^2} \left(1 + \frac{1}{2} \rho^2 + \frac{3}{8} \rho^4 \right), \quad (4)$$

with $p_0 = 7W/(6\pi a^2)$, results in the indentation by a axi-symmetric punch bounded by a sixth-order polynomial surface:

$$hi(r) = \frac{15}{2048} \pi \eta p_0 a \cdot \left[24 \left(\frac{r}{a} \right)^2 + 6 \left(\frac{r}{a} \right)^4 + 5 \left(\frac{r}{a} \right)^6 \right]. \quad (5)$$

3. Contact model

The contact model employed in this paper is similar with the one presented in [8], consisting in three type of equations: (1) the equation of the surface of deformation between the two bodies, (2) the boundary conditions, and (3) the static equilibrium.

The difficulty in solving the contact model stems from the fact that neither the contact area, nor the pressure distribution are known in advance, and moreover, keep changing during the contact process, together with the compliance of the viscoelastic material. The numerical treatment of the aforementioned contact involves therefore a spatial discretization of the contact surface, as well as an additional temporal discretization. The spatial discretization employs a rectangular uniform mesh laying in the common plane of contact, on which all problem parameters are assumed piecewise-constant, based on the discrete values computed in the control points. The temporal discretization assumes that the

loading window $[0, t]$ is divided into small time steps, and the problem parameters are assumed piecewise-constant in the time dimension as well.

The main advantage of this discretization process is the substitution of integration of arbitrary functions over arbitrary spatial or temporal domains with summation, which can be performed for prescribed input. The notation of problem parameters can then make use of the discrete indexes covering the discrete surface patches, i.e. $p(i, j, k)$ is the uniform pressure predicted for the patch (i, j) of the surface spatial grid, after k time steps.

Within this framework, a solution for the viscoelastic displacement induced by a prescribed, but otherwise arbitrary loading history, at a prescribed time in the observation window, is readily available [7]:

$$u_3^{vs}(i, j, k) = \sum_{n=1}^{N_t} \sum_{l=1}^{N_1} \sum_{m=1}^{N_2} K_{vs}(i-1, j-m, k-n) \times (p(1, m, n) - p(1, m, n-1)),$$

$$i = 1K N_1, j = 1K N_2, k = 1K N_t, \quad (6)$$

where N_1 and N_2 are the number of spatial grids and N_t the number of temporal steps.

$K_{vs}(i-1, j-m, k-n)$ denotes the viscoelastic influence coefficient [7], expressing the displacement induced after k time steps in the spatial cell (i, j) , by a uniform pressure of magnitude $1/(\Delta_1 \Delta_2) Pa$, that acted in the cell $(1, m)$ in the n^{th} time step of the observation window, with $n \leq k$. Equation (6) proves that viscoelastic displacement computation requires the entire history of pressure distribution in the viscoelastic contact.

To overcome the memory effect specific to viscoelastic materials, the contact model is solved successively at every time step, thus assuring the simulation of the loading history. The contact solver is based on the Conjugate Gradient-type scheme originally advanced by

Polonsky and Keer [6] for the elastic contact of rough surfaces.

In the beginning of the observation window, no loading history is assumed, so the initial contact state is calculated as a purely elastic process, i.e. the initial displacement is generated by the current pressure only. In the subsequent time increments, the pressure history, which is obtained in a step-by-step approach, is superimposed in the equation of the surface of deformation.

The instantaneous contact area and pressure distribution are determined with a trial-and-error approach. A guess contact region is assumed, and the resulting pressure distribution is then computed based on this assumption. If all constraints in the contact model are verified, a contact problem solution is achieved. This solution is unique based on the theorem of uniqueness of solution for the elastostatic problem. Otherwise, the process is restarted with a different initial guess.

4. Results and discussions

The general formulae for the contact of high-order surfaces, optimized for a central plateau of uniform pressure, are first verified numerically. The pressure profiles in a radial plane, depicted in figure 1, induced by axisymmetric punches of eqs (2) and (5), match well their analytical counterparts (3) and (4), respectively. Dimensionless pressure is defined as ratio to p_H , the central pressure obtained when the same load is transmitted through the same contact area in a Hertz-type indentation. Dimensionless radial coordinate is defined as ratio to the contact area a , which is fixed but otherwise can be arbitrarily chosen. The normal load, as well as the contact compliance, are also fixed.

The pressure profiles in figure 1 prove clearly that, when the same normal load is transmitted through the same contact area, the use of optimized high-order polynomial punches lead to a more uniform pressure distribution. The latter is expected to improve the load-carrying capacity of the mechanical contact.

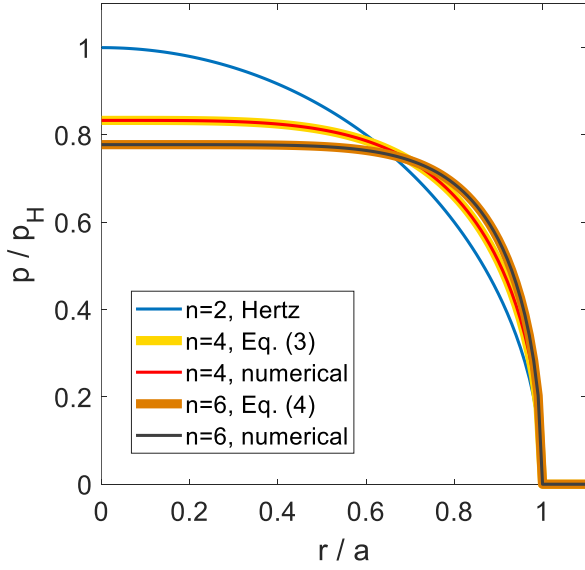


Figure 1: The elastic contact of high-order surfaces

The constitutive law of the viscoelastic material employed in this paper is that of the polymethyl methacrylate (PMMA), a thermoplastic polymer whose relaxation modulus under uniaxial compression in a window of observation of 1000 s was obtained experimentally by Kumar and Narasimhan [9]. The creep compliance of PMMA, needed in the computation of the influence coefficients K_{vs} , results by inverse Laplace transform, as described in [10]:

$$\Phi(t) = 7 \cdot 10^{-4} - 6.17 \cdot 10^{-5} \exp(-0.1t) - 8.38 \cdot 10^{-5} \exp(-7.47 \cdot 10^{-3}t), [1/\text{MPa}]. \quad (7)$$

The viscoelastic part of the computer program was benchmarked against the implicit solutions derived in the classical literature [11-15] of the viscoelastic contact. The step loading spherical indentation of a viscoelastic half-space described by the Maxwell rheological model with the relaxation time τ is analyzed in figure 2. The Hertz contact parameters (contact radius a_H , central pressure p_H), are used as normalizers. The pressure profiles achieved at various time moments from the loading history agree well with the classic solution.

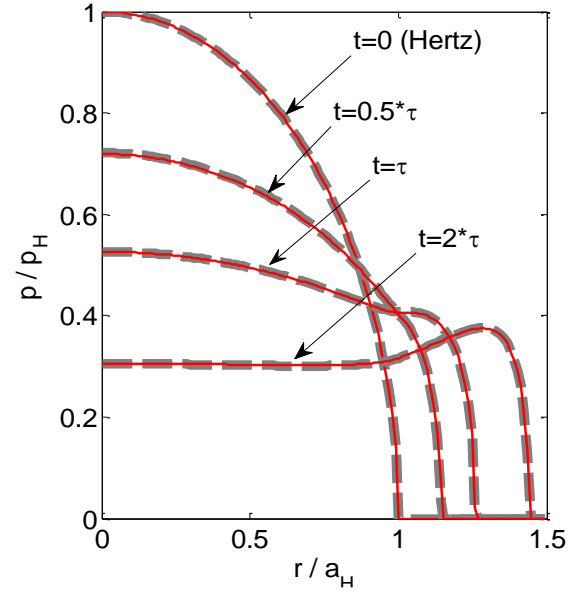


Figure 2: Maxwell half-space spherical indentation: continuous lines - analytical data; dashed lines – numerical predictions

Figure 3 shows the pressure profiles attained in the indentation of a PMMA viscoelastic half-space indented by a rigid fourth-order polynomial punch of equation (2), whereas the results for the sixth-order surface given by eq. (5), are shown in figure 4. The radial coordinate is normalized by the contact radius achieved at the beginning of the loading process (i.e., at $t=0$), and pressure distribution by the initial maximum (central) pressure.

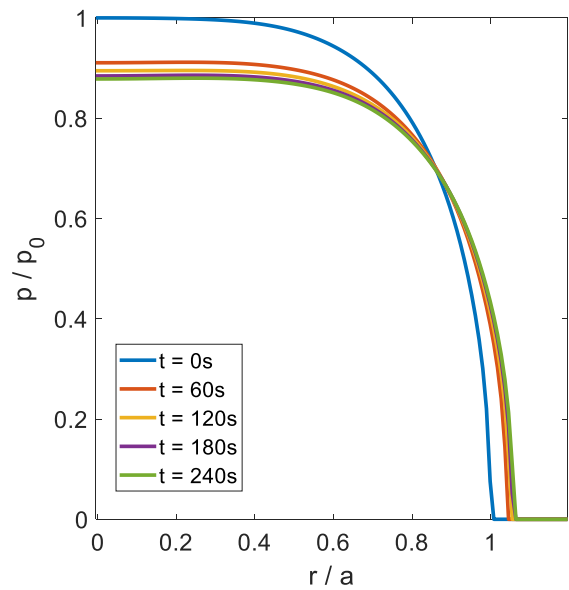


Figure 3: PMMA fourth-order polynomial punch indentation

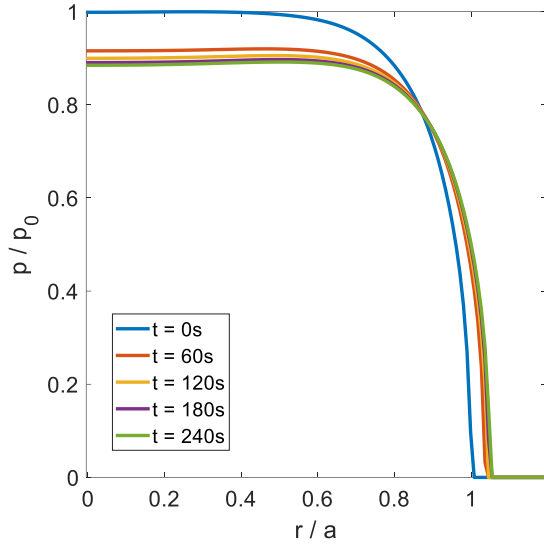


Figure 4: PMMA sixth-order polynomial punch indentation

The radial pressure profiles in figures 4 and 5 suggest that the central plateau of uniform pressure extends with time, while the contact area increases, as depicted in figure 5. Dimensionless contact area is defined as ratio to the initial contact area $A_0 = \pi a^2$.

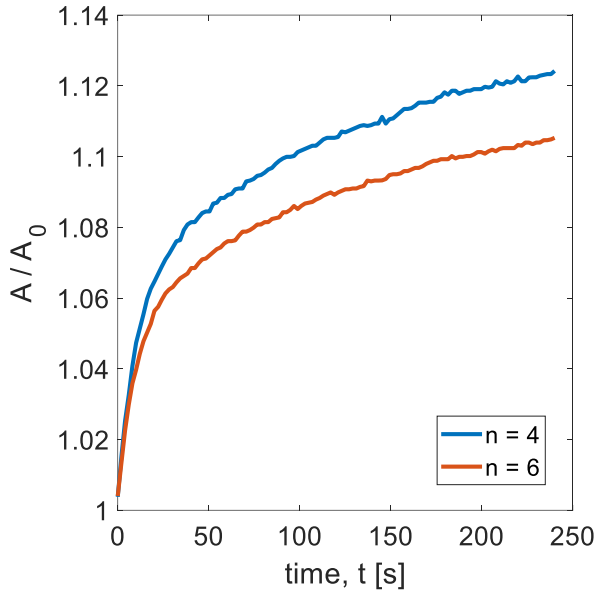


Figure 5: Evolution of contact area

The evolution of the rigid-body approach is presented in figure 6. The normal approach is normalized by the initial (i.e., at $t=0$) value ω_0 , which is different for each n . The same trend as for the contact area can be observed.

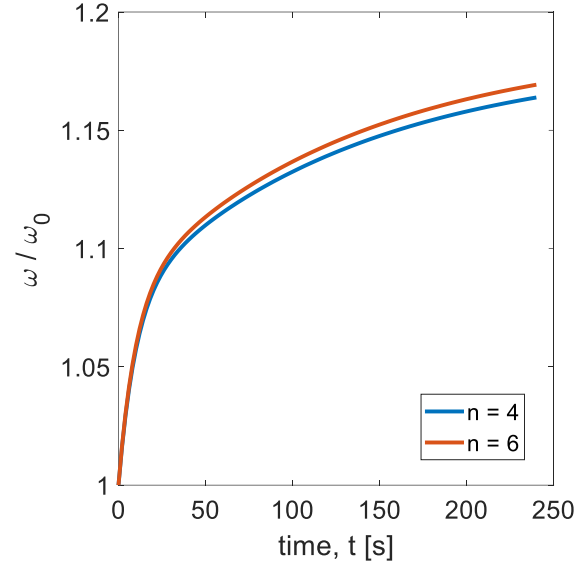


Figure 6: Evolution of dimensionless rigid-body approach

5. Conclusions

The simulation of the contact of linear viscoelastic bodies, bounded by high-order polynomial surfaces, is achieved in this paper by combining a robust solver for the frictionless normal contact with a numerical method for the calculation of the displacement induced in a viscoelastic half-space by a prescribed but otherwise arbitrary pressure history. The method requires both spatial and temporal discretization. The viscoelastic contact process simulation is accomplished by computing a series of subsequent contact states.

Code validation is achieved by comparison with the contact of complex geometries in the purely elastic domain, or with that of simple geometries of viscoelastic bodies described by basic rheological models.

The initial plateau of uniform pressure specific to optimized high-order polynomial surfaces is conserved and extended during the loading program. Contact area also increases with time, particularly when the degree of the polynomial is smaller.

The numerical simulations suggest that the high-order surfaces are also attractive for the contact in the viscoelastic domain, conserving a close to uniform pressure in the center of the contact area.

6. Acknowledgement

This work was partially supported from the project “Integrated Center for Research, Development and Innovation in Advanced Materials, Nanotechnologies, and Distributed Systems for Fabrication and Control”, Contract No. 671/09.04.2015, Sectoral Operational Program for Increase of the Economic Competitiveness co-funded from the European Regional Development Fund.

7. References

- [1] Hasslinger, J., 1992, *Contact shape optimisation: the mathematical theory*, Proceedings of the Contact Mechanics International Symposium, A. Curier (Ed.), pp. 287–303, Presses Polytechniques et Universitaires Romandes, Laussane, Switzerland.
- [2] Diaconescu, E., 2006, *Elliptic elastic contact between high order symmetrical surfaces*, ASME J. Tribol., 128(4), 908-914.
- [3] Diaconescu, E., and Glovnea, M., 2005, *Flat Central Pressure in Circular Elastic Contacts Between High Order Surfaces*, Proceedings of WTC2005, World Tribology Congress III, September 12-16, 2005, Washington, D.C., USA, Article ID WTC2005-63647.
- [4] Glovnea, M., Spinu, S., and Diaconescu, E., 2012, *Improved pressure distribution in elliptic elastic contacts between high-order surfaces*, Advances in Tribology, Vol. 2012, Article ID 832859, 11 pp.
- [5] Spinu, S., and Gradinaru, D., 2013, *Numerical Analysis of Load Carrying Capacity in the Contact between High-Order Surfaces*, Applied Mechanics and Materials, Vol. 371, pp. 571-575.
- [6] Polonsky, I. A., and Keer L. M., 1999, *A Numerical Method for Solving Rough Contact Problems Based on the Multi-Level Multi-Summation and Conjugate Gradient Techniques*, Wear, **231**(2), pp. 206-219.
- [7] Spinu, S., and Gradinaru, D., 2015, *Semi-Analytical Computation of Displacement in Linear Viscoelastic Materials*, IOP Conf. Ser.: Mater. Sci. Eng. **95**, 012111 (7 pages).
- [8] Spinu, S., 2015, *Numerical Simulation of Viscoelastic Contacts. Part I. Algorithm Overview*, J. Balk. Tribol. Assoc., **21**(2), pp. 269-280.
- [9] Kumar, M. V. R., and Narasimhan, R., 2004, *Analysis of Spherical Indentation of Linear Viscoelastic Materials*, Curr. Sci., **87**, pp. 1088-1095.
- [10] Chen, W. W., Wang, Q. J., Huan, Z., and Luo, X., 2008, *Semi-Analytical Viscoelastic Contact Modeling of Polymer-Based Materials*, ASME J. Tribol., **133**(4), 041404 (10 pages).
- [11] Lee, E. H., and Radok J. R. M, 1960, *The Contact Problem for Viscoelastic Bodies*, ASME J. Appl. Mech., **27**(3), pp. 438-444.
- [12] Hunter, S. C., 1960, *The Hertz Problem for a Rigid Spherical Indenter and a Viscoelastic Half-Space*, J. Mech. Phys. Solids, **8**(4), pp. 219-234.
- [13] Yang, W. H., 1966, *The Contact Problem for Viscoelastic Bodies*, ASME J. Appl. Mech., **33**(2), pp. 395-401.
- [14] Ting, T. C. T., 1966, *The Contact Stresses Between a Rigid Indenter and a Viscoelastic Half-Space*, ASME J. Appl. Mech., **33**(4), pp. 845-854.
- [15] Ting, T. C. T., 1968, *Contact Problems in the Linear Theory of Viscoelasticity*, ASME J. Appl. Mech., **35**(2), pp. 248-254.